

See discussions, stats, and author profiles for this publication at: <https://www.researchgate.net/publication/231528239>

Unimolecular Chemistry of the Gaseous Cyclopropylamine Radical Cation

ARTICLE *in* JOURNAL OF THE AMERICAN CHEMICAL SOCIETY · JANUARY 1998

Impact Factor: 12.11 · DOI: 10.1021/ja971724m

CITATIONS

20

READS

38

4 AUTHORS, INCLUDING:



Guy Bouchoux

Université Paris-Sud 11

231 PUBLICATIONS 2,804 CITATIONS

SEE PROFILE



Minh Tho Nguyen

University of Leuven

748 PUBLICATIONS 10,835 CITATIONS

SEE PROFILE

Unimolecular Chemistry of the Gaseous Cyclopropylamine Radical Cation

Guy Bouchoux,^{*,†} Christian Alcaraz,[‡] Odile Dutuit,[§] and Minh Tho Nguyen[⊥]

Contribution from the Laboratoire des Mécanismes Réactionnels, UA CNRS 1307, Ecole Polytechnique, 91128 Palaiseau Cedex, France, Laboratoire pour l'Utilisation du Rayonnement Electromagnétique (LURE), Bât. 209D, Université Paris-Sud, 91405 Orsay, France, Laboratoire de Physicochimie des Rayonnements, Bât. 350, Université Paris-Sud, 91405 Orsay, France, and Department of Chemistry, University of Leuven, Celestijnenlaan 200F, 3001 Leuven, Belgium

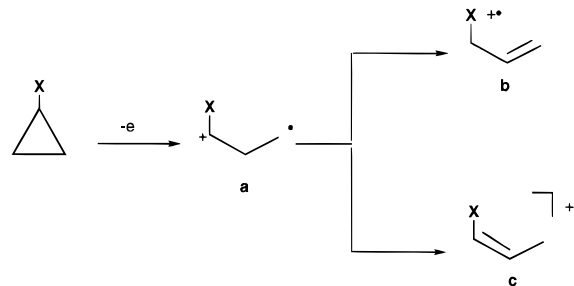
Received May 27, 1997[⊗]

Abstract: The rearrangement–dissociation mechanisms of ionized cyclopropylamine have been studied with tandem mass spectrometry, photoion–photoelectron coincidence spectroscopy, and (PU)MP4SDTQ/6-311G**/MP2/6-31G*+ZPE molecular orbital calculations. The present investigation demonstrates that the cyclic structure of cyclopropylamine is not preserved after electron removal; in fact, photon or electron ionization leads to a more stable open form, $[\text{CH}_2\text{CH}_2\text{CHNH}_2]^+$, **2**, which belongs to the category of distonic ions. Dissociative ionization of cyclopropylamine leads essentially to H atom loss. Experiments demonstrate that (i) the dissociation threshold is compatible only with the $[\text{CH}_2\text{CHCHNH}_2]^+$ fragment ion structure, (ii) the hydrogen expelled from ions of low internal energy comes exclusively from a carbon, and (iii) the dissociation rate exhibits a very slow rise with internal energy. Molecular orbital calculations predict that the lowest energy pathway involves isomerization of **2** into ionized 1-aminopropene, $[\text{CH}_3\text{CHCHNH}_2]^+$, **3**. The degenerate 1,2-HCNH₂ shift $[\text{CH}_2\text{CH}_2\text{CHNH}_2]^+$, **2** \rightleftharpoons $[\text{NH}_2\text{CHCH}_2\text{CH}_2]^+$, **2**, is found to require a negligible critical energy. A statistical (RRKM) modeling of the reaction rate accurately reproduces the experimental data, and the observed slow down effect on the dissociation rate appears to be due to the passage through the very stable structure **3**. Several previously unknown thermochemical parameters, including the standard heat of formation of various neutral and ionized (C₃, H₇, N) species, are proposed; for example $\Delta_f H^\circ_{300}[\text{CH}_2\text{CH}_2\text{CHNH}_2]^+ = 840 \pm 10$ kJ/mol and $\Delta_f H^\circ_{300}[\text{CH}_3\text{CHCHNH}_2]^+ = 770 \pm 10$ kJ/mol are deduced from a combination of experiment and theory.

Introduction

The cyclopropyl group holds an important place in organic chemistry and, as a result, the behavior of molecules containing this functional group has been extensively described.¹ By contrast, the reactivity of the corresponding radical cations, either in solution or in the gas phase, is only barely documented. A constant feature seems to emerge from examination of the data presently available:² upon removal of one electron, cyclopropane derivatives specifically undergo ring opening by cleavage of the C(1)–C(2) bond (Scheme 1). The distonic radical cation **a** so produced may, in a subsequent step, give rise to species **b** or **c** by 1,2-hydrogen migrations.

Scheme 1



The branching ratio **b/c** seems to be largely substituent dependent. For example, isomer **b** is exclusively produced from alkyl-substituted cyclopropanes. The situation is more evenly balanced for ethers or halogen derivatives, for which both **b** and **c** are competitively formed, but to date, the nature of these substituent effects remains to be established.

The facile formation of ion **a** also raises the question of the existence of the ionized cyclic structure as a stable species. Accordingly, ionized cyclopropanol must be seen as a transition structure rather than a minimum in the $[\text{C}_3\text{H}_6\text{O}]^+$ potential energy surface.^{2d,f,h} It has been recently demonstrated that ionized cyclobutanol and cyclobutylamine are not stable and spontaneously rearrange to a stable distonic structure by C(1)–C(2) bond cleavage.³ Thus, the behavior of cyclopropyl derivatives parallels that of substituted cyclobutanes.

[†] Ecole Polytechnique.

[‡] Laboratoire pour l'Utilisation du Rayonnement Electromagnétique, Université Paris-Sud.

[§] Laboratoire de Physicochimie des Rayonnements, Université, Paris-Sud.

[⊥] University of Leuven.

[⊗] Abstract published in *Advance ACS Abstracts*, December 15, 1997.

(1) Rappoport, Z., Ed. *The Chemistry of the Cyclopropyl Group*; John Wiley: New York, 1987.

(2) (a) Hammerum, S. *Mass Spectrom. Rev.* **1988**, *7*, 123. (b) Bouchoux, G. *Mass Spectrom. Rev.* **1988**, *7*, 1 and 203. (c) Burgers, P. C.; Terlouw, J. K. In *Specialist Periodical Reports: Mass Spectrometry*; Rose, M. E., Ed.; The Royal Society of Chemistry: London, 1989. (d) Bouchoux, G. *Adv. Mass Spectrom.* **1989**, *11A*, 812. (e) Schwarz, H. In ref 1, p 173. (f) Bouchoux, G.; Tortajada, J. *Rapid Commun. Mass Spectrom.* **1987**, *1*, 86. (g) Polce, M. J.; Wesdemiotis, C. *J. Am. Soc. Mass Spectrom.* **1996**, *7*, 573. (h) Bouchoux, G.; Luna, A.; Tortajada, J. *Int. J. Mass Spectrom. Ion Proc.* In press.

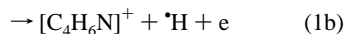
There is also evidence for ring opening of the cyclopropylamine radical cation in solution^{4,5} and in the gas phase.⁶ It is often postulated that this reaction is implicated in the mechanism of inactivation of monoamine oxidase and cytochrome P-450 by cyclopropylamine.⁴ In an ESR study devoted to this question, it has been concluded that both ionized cyclopropylamine^{5a} and allylamine^{5b} isomerize into the distonic structure **a**; however, the possible formation of ions of type **c** has not been considered.

It is therefore of interest to investigate the cyclopropylamine system by using accurate experimental and theoretical methods in order to answer the following questions: Is the cyclopropylamine radical cation a stable structure? What are the relative energies of the isomers **a**, **b**, and **c**? What isomerization routes are available for these species? What are their dissociation characteristics? For this purpose we use tandem mass spectrometry and photoion-photoelectron spectrometry in conjunction with high level molecular orbital calculations.

Experimental Procedures and Computational Details

A. The photoionization apparatus has been fully described in a previous publication.⁷ Ions are produced by photoionization with synchrotron radiation at Super-ACO, the Orsay storage ring. The VUV light is dispersed by a 3m, normal incidence, Balzers monochromator equipped with a 1200 lines/mm Jobin-Yvon holographic grating and a LiF window to suppress the contribution of second-order light for photon energies below 11.85 eV. The monochromatized light is refocused at the center of the ion source where the gaseous sample is introduced at an indicated pressure of 10^{-4} mbar. Electrons and ions are extracted in opposite directions by an electric field of ca. 2.5 V/cm. Angular and time discrimination allows the exclusive detection of threshold photoelectrons (i.e. electrons with a kinetic energy of less than 15 meV). The remainder of the ion assembly includes a double octopole ion guide, a quadrupole mass filter, and a multichannel plate analyzer.

During a photoionization process, $M + h\nu \rightarrow [M]^+ + e$, the measurement of the signal corresponding to the molecular ion or to the ejected electron as a function of photon energies allows the ionization energy of the molecule to be determined. Similarly, the appearance energy of the fragment ions $[A]^+$ coming from $M + h\nu \rightarrow [A]^+ + N + e$ may be obtained from either the direct photoion signal or the threshold photoelectron-photoion signal. We used this procedure here to analyze the energetics of the photoionization and photodissociation of cyclopropylamine (eqs 1a and 1b):



B. Unimolecular dissociations of metastable ions were studied in the second Field Free region of a VG.ZAB.2F B-E mass spectrometer working in the Mass Analyzed Ion Kinetic Energy (MIKE) mode. Typical instrument conditions were the following: filament current = 100 μA , ionizing energy = 70 eV, source temperature = 170 $^\circ\text{C}$, and

accelerating voltage = 8 kV. The kinetic energy values were calculated after correction for the width of the main beam.

C. Ab initio molecular orbital calculations were carried out with a local version of the GAUSSIAN 92 program.⁸ Geometries of the structures considered were first optimized at the (unrestricted) Hartree-Fock level with the 6-31G* basis set. Harmonic vibrational frequencies were computed at this level in order to characterize the structures and to estimate zero point vibrational energies (ZPE). Improved geometries were subsequently obtained through calculations using correlated wave functions at the second-order Møller-Plesset perturbation theory (MP2) level with the 6-31G* basis set. Finally, relative energies were refined by using the 6-311G** basis set and (U)MP4SDTQ theory. In some structures the spin contamination present in UHF references is substantial ($\langle S_z \rangle \geq 0.8$). To account for the effect of spin contamination on the convergence of the UMP4 perturbation expansion, we have applied a projection technique at the fourth-order (PUMP4) and, for some points, a quadratic configuration interaction including all single and double substitutions and estimates for triple substitutions (QCISD-(T)/6-311G(d,p)). Unless otherwise noted, the relative energies referred to in the text correspond to our uniform estimates obtained at the (PU)-MP4SDTQ/6-311G**//MP2/6-31G*+ZPE level. Corresponding total and zero-point energies are given in Table 1. Relevant geometrical parameters of some structures of interest, as optimized at the MP2/6-31G* level, are presented in Chart 1 (bond length in angstroms and bond angles in degrees); the data concerning the other structures presented in Table 1 are available upon request from the authors.

Results and Discussion

As far as notation is concerned, we employ hereafter **1n** and **3n-6n** to designate the neutral species whereas **1-9** stand for the corresponding radical cations. In general **X/Y** designates a transition structure (TS) connecting both ions **X** and **Y** (**X**, **Y** for **1** to **9**).

A. Experimental Results. (i) Dissociations of Cyclopropylamine Radical Cations. The conventional 70 eV electron impact mass spectrum of cyclopropylamine **1n** exhibits five prominent peaks: m/z 57 ($[\text{C}_3\text{H}_7\text{N}]^{*+}$), 56 ($[\text{C}_3\text{H}_6\text{N}]^+$, **[1-H]**⁺), 30, 29, and 28. At lower ionizing energies only the two former signals are significant: the behavior of $[\text{C}_3\text{H}_7\text{N}]^{*+}$ ions of low internal energy generated from cyclopropylamine is dominated by the reaction $[\text{C}_3\text{H}_7\text{N}]^{*+} \rightarrow [\text{C}_3\text{H}_6\text{N}]^+ + \text{H}^\cdot$.

These findings are confirmed under our conditions of photoionization experiments. Accordingly, at a photon energy of 21.21 eV the photoionization mass spectrum of cyclopropylamine is dominated by one peak, at m/z 56; other signals are observed at m/z 28, 29, 30, and 57 which amount to 80%, 20%, 40%, and 25%, respectively, of the base peak m/z 56. When the photon energy is further reduced, the m/z 29 peak rapidly disappears and then the m/z 28 and 30 signals. For example at 11.5 eV, the four peaks m/z 28, 30, 56, and 57 are detected in the intensity ratio 2/15/100/20. Below 10.5 eV the only significant signals are those associated with $[\text{C}_3\text{H}_7\text{N}]^{*+}$ and $[\text{C}_3\text{H}_6\text{N}]^+$ ions.

The fact that metastable $[\text{C}_3\text{H}_7\text{N}]^{*+}$ ions (i.e. species of lifetime $\approx 10^{-5}$ s) produced by electron ionization of cyclopropylamine eliminate exclusively a hydrogen atom is established from its MIKE spectrum, which presents only one peak at m/z 56. Moreover, when using the cyclopropylamine-ND₂ derivative (obtained by H/D exchange between cyclopropylamine and D₂O in the inlet system of the VG-ZAB-2F mass spectrometer), two signals are observed at m/z 58 (100%) and

(3) Bouchoux, G.; Alcaraz, C.; Dutuit, O.; Nguyen, M. T. *Int. J. Mass Spectrom. Ion Proc.* **1994**, 137, 93.

(4) (a) Banik, G. M.; Silverman, R. B. *J. Am. Chem. Soc.* **1990**, 112, 4499. (b) Woo, J. C. G.; Silverman, R. B. *J. Am. Chem. Soc.* **1995**, 117, 1663. (c) Zhong, B.; Silverman, R. B. *J. Am. Chem. Soc.* **1997**, 119, 6690.

(5) (a) Qin, X. Z.; Williams, F. J. *Am. Chem. Soc.* **1987**, 109, 595. (b) Dai, S.; Guo, Q. X.; Wang, J. T.; Williams, F. J. *Chem. Soc., Chem. Commun.* **1988**, 1069.

(6) Bouchoux, G.; Flament, J. P.; Hoppilliard, Y.; Tortajada, J.; Flam-mang, R.; Maquestiau, A. *J. Am. Chem. Soc.* **1989**, 111, 5560.

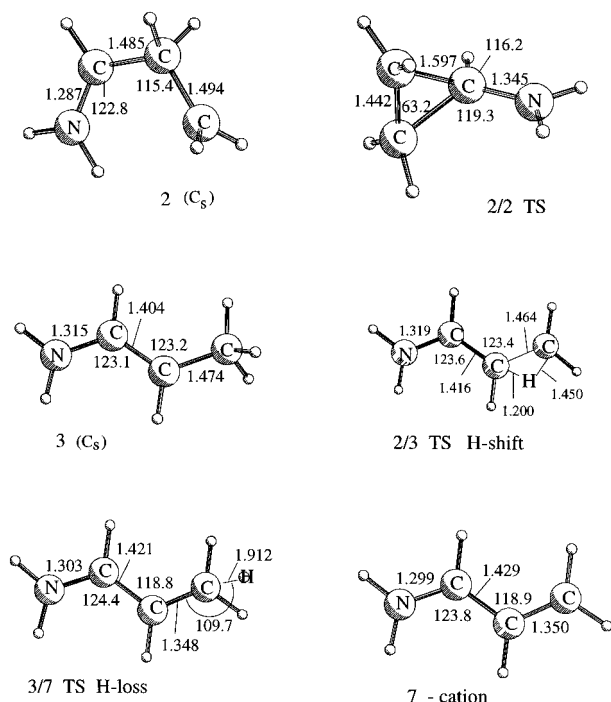
(7) (a) Metayer-Zeitoun C. Doctoral Thesis, July 1992, University of Orsay. (b) Dutuit, O. In *Fundamentals of Gas Phase Ion Chemistry*; Jennings, K., Ed.; Kluwer Academic Publisher: Dordrecht, The Netherlands, 1991; p 21. (c) Alcaraz, C.; Dutuit, O.; Gerlich, D.; Guyon, P. M.; Hepburn, J.; Metayer-Zeitoun, C.; Ozenne, J. B.; Schweizer, M.; Weng, T. *Chem. Phys.* **1996**, 209, 177.

(8) Program GAUSSIAN 92, Frisch, M. J.; Trucks, G. W.; Head-Gordon, M.; Gill, P. M. W.; Wong, M. W.; Foresman, J. B.; Johnson, B. G.; Schlegel, H. B.; Robb, M. A.; Replogle, E. S.; Gomperts, R.; Andres, J. L.; Raghavachari, K.; Binkley, J. S.; Gonzalez, C.; Martin, R. L.; Fox, D. J.; Defrees, D. J.; Baker, J.; Stewart, J. J. P.; Pople, J. A. Gaussian Inc., Pittsburgh, PA, 1991.

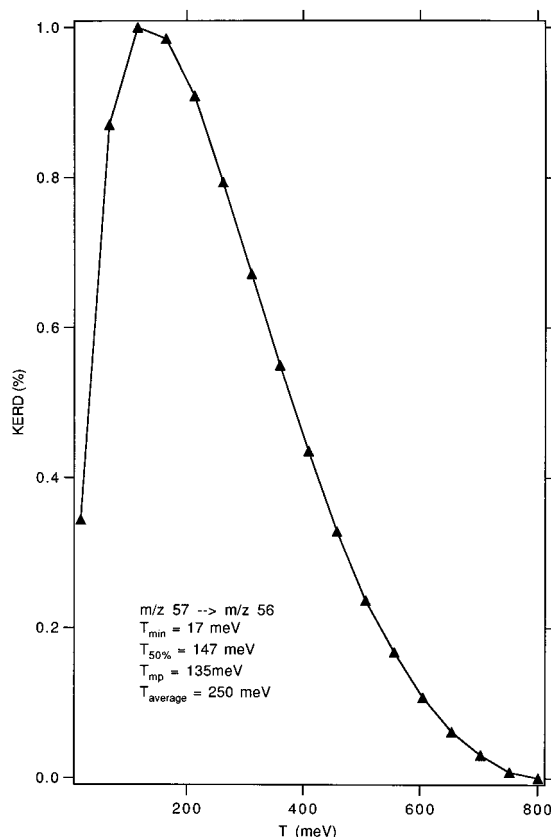
Table 1. Relative Energies (kJ/mol), Zero-Point Vibrational Energies (kJ/mol), and Expectation Values of Spin Squared for Neutral and Ionized C₃H₇N Species^a

structure	UMP2(F)/6-31G(d) ^b	UMP4SDTQ/6-311G(d,p) ^c	PUMP4SDTQ/6-311G(d,p) ^d	ZPE ^e	STE ^f	$\langle S^2 \rangle$
1n	-727	-746	-738	252	261	
3n		-785	-782	247		
4n		-759	-754	249		
5n		-806	-803	247		
6n		-655	-653	246		
1 (vertical)		170	169	177	252	0.762
2	0	0	0	0 (0)	244	0.762
3	-68	-67	-73	-65 (-65)	248	0.808
4	89	78	74	73	243	0.782
5	104	95	87	82	239	0.811
6	47	45	42	44	246	0.780
7 + H⁺	104	137	140	120 (120)	224	0.750
8 + H⁺	132	167	170	143	217	0.750
9 + C₂H₄	266	249	243	229	230	0.808
2/2	18	23	21	23	246	0.775
2/3	114	107	102	93 (97)	235	0.804
2/4	145	136	127	117	234	0.833
2/5	159	145	132	121	233	0.837
2/6	186	175	173	166	237	0.773
3/6	189	177	177	167		0.765
5/6	294	276	273	254	234	0.786
2/7	177	186	161	143 (150)	226	1.037
3/7	145	162	142	124 (131)	226	0.980
4/7		177	168	150	226	0.803
5/8	218	219	201	176	219	0.885

^a Based on MP2/6-31G(d) optimized geometries. ^b Total energy of structure **2**: -172.37585 hartrees. ^c Total energy of structure **2**: -172.53610 hartrees. ^d Total energy of structure **2**: -172.53729 hartrees, relative energies corrected for the ZPE are indicated in bold face. The QCISD(T)/6-311G(d,p)+ZPE values are given in parentheses: at that level, the total energy of structure **2** is -172.53883 hartrees. ^e Zero point vibrational energies calculated from UHF/6-31G(d) normal modes and scaled by a factor of 0.9. ^f Sum of thermal energies at 300 K (UHF/6-31G(d) calculations scaled by 0.9, including the term $5/2RT$ for H).

Chart 1

m/z 57 (1%) in the MIKE spectrum of m/z 59 ions, indicating a quasispecific H atom elimination. These dissociations, together with the m/z 57 \rightarrow m/z 56 metastable ion decomposition observed for unlabeled cyclopropylamine, are characterized by identical kinetic energy release distributions (KERD). The KERD derived from the analysis of the metastable peak profiles⁹ is presented in Figure 1.

**Figure 1.** Kinetic energy release distribution of the experimental m/z 57 \rightarrow m/z 56 metastable ion decomposition from cyclopropylamine.

The distribution spans from $T_{\min} = 15 \pm 5$ meV to $T_{\max} \approx 800$ meV and is characterized by an average T value $T_{\text{average}} = 250 \pm 20$ meV (24 kJ/mol) and by a most probable value $T_{\text{mp}} = 135 \pm 10$ meV. We also note that the CID spectrum

(9) Holmes, J. H.; Osborne, A. D. *Int. J. Mass Spectrom. Ion Phys.* **1977**, 23, 189.

of m/z 59 ions of the cyclopropylamine-ND₂ derivative presents two peaks at m/z 58 and 57 in the approximate ratio 100/2. This ratio is very close to that observed in the MIKE spectrum and consequently demonstrates that internal energy has little effect, if any, in the (H loss)/(D loss) branching ratio.

It should be recalled at this stage that previous collisional experiments⁶ have demonstrated that the $[C_3H_6N]^+$ ions generated from cyclopropylamine, either in the source or in the second field free of the mass spectrometer, has a vinyliminium structure, $[CH_2=CHCH=NH_2]^+$. This point will be further confirmed by the measurement of the corresponding threshold energy.

The loss of H is also the exclusive dissociation observed from ionized allylamine $[CH_2=CHCH_2NH_2]^+$. Metastable ions dissociate with a kinetic energy release comparable to what has been noted for cyclopropylamine (characteristics of the KERD: $T_{\min} = 15 \pm 5$ meV, $T_{\max} \approx 800$ meV, and $T_{\text{average}} = 250 \pm 20$ meV). The metastable molecular ion of ND₂-allylamine also eliminates essentially an H atom (100%) rather than a D atom (0.5%).

(ii) Determination of the Onset Energies by Photoionization. The experimental threshold energies for the appearance of a given ion may be derived from photoionization experiments by linear extrapolation of the first rising portion of the relevant ionization efficiency curve to the abscissa. The curve of the fragment ion abundance versus photon energy allows the determination of the appearance energy, $AE[\text{fragment ion}]^+$. In the case of the ionization energy, $IE(\mathbf{1n})$, the threshold photoelectron intensity versus photon energy curve has been used, instead of the parent ion abundance, in order to have a better sensitivity in the measurement. The apparent, 300 K, threshold energies are $IE_{300}(\mathbf{1n}) = 8.78 \pm 0.03$ eV and $AE_{300}[C_3H_6N]^+ = 9.32 \pm 0.05$ eV. Our ionization energy value, $IE_{300}(\mathbf{1n})$, agrees well with the values determined from He I photoelectron spectroscopy, i.e. 8.7 eV¹⁰ and 8.85 ± 0.09 eV,¹¹ both values reported as onset of the photoelectron band. It has been established that a photoionization threshold energy at a temperature T will be less than that at 0 K by a quantity which, under the assumption of a linear photoionization efficiency law, is the average internal thermal energy $\langle E \rangle_T$ of the molecule.¹² The correction for the thermal energy may be obtained by using a Boltzman distribution, where the probability of a given internal energy is proportional to $N(E) \exp(-E/kT)$ in which k represents the Boltzmann constant and $N(E)$ the density of vibrational-rotational states of the molecule. The resulting average thermal energy of cyclopropylamine at 300 K, $\langle E \rangle_{300}$, was calculated to be 0.08 eV. The density of states $N(E)$ was obtained with use of the Stein-Rabinovitch algorithm¹³ with vibrational wave-numbers given by molecular orbital calculations (HF/6-31G*, scaled by a factor of 0.91²²). Consequently the corrected 0 K, threshold energies are $IE_0(\mathbf{1n}) = 8.86 \pm 0.03$ eV and $AE_0[C_3H_6N]^+ = 9.40 \pm 0.05$ eV.

Another, more accurate way of measuring the dissociative photoionization onset is to use the breakdown graph obtained by the photoelectron-photoion coincidence technique.¹⁴ The experiment consists of monitoring the signals of the parent m/z

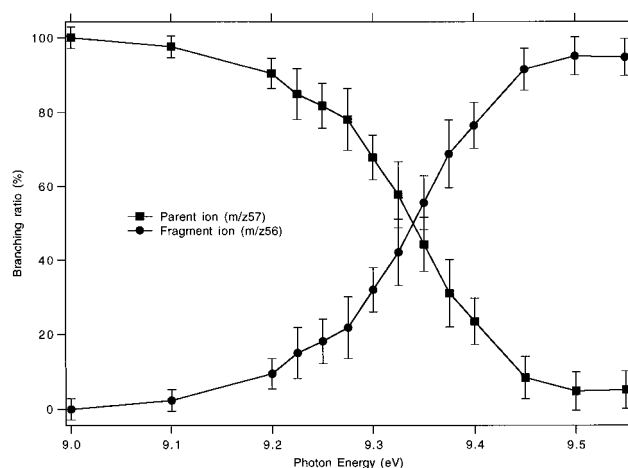


Figure 2. Breakdown graph of cyclopropylamine in the vicinity of the H loss channel.

57 and the daughter m/z 56 ions in coincidence with electrons of zero energy as a function of the photon energy. The plot of the fractional abundances of $[C_3H_7N]^+$ and $[C_3H_6N]^+$ ions as a function of the photon energy (the so-called breakdown graph) is shown in Figure 2.

The dissociation onset may be obtained from the crossover point of this breakdown graph. At the crossover energy C_{300} , half of the parent ions have enough energy to dissociate. This corresponds to half of the population of precursor molecules and thus to the median energy in the thermal energy distribution. The onset energy at 0 K (C_0) is obtained simply by adding the mean thermal energy (which is close to the average value $\langle E \rangle_{300} = 0.08$ eV, see above) to the crossover energy C_{300} . The C_{300} and C_0 values for H loss from cyclopropylamine were found to be 9.34 ± 0.02 and 9.42 ± 0.02 eV, respectively, in good agreement with the AE_{300} and AE_0 of 9.32 ± 0.05 and 9.40 ± 0.05 eV, determined by the linear extrapolation described above.

It is now interesting to compare the experimental determinations of the appearance energy of the fragment ions $[C_3H_6N]^+$ with the known thermochemistry of the fragmentation processes. For the dissociation $[\mathbf{1}]^{++} \rightarrow [C_3H_6N]^+ + \cdot H$, a maximum value for the 300 K heat of formation of the product ions is given by eq 2:

$$\Delta_f H^\circ_{300}[C_3H_6N]^+ = AE_0[C_3H_6N]^+ - \Delta_f H^\circ_{300}(\cdot H) + \Delta_f H^\circ_{300}(\mathbf{1n}) \quad (2)$$

Using the previously determined $AE_0 = 9.42$ eV (909 kJ/mol) together with $\Delta_f H^\circ_{300}(\cdot H) = 218$ kJ/mol¹⁰ and $\Delta_f H^\circ_{300}(\mathbf{1n}) = 77$ kJ/mol,¹⁵ one obtains $\Delta_f H^\circ_{300}[C_3H_6N]^+ \leq 768$ kJ/mol, a value that is compatible only with two $[C_3H_6N]^+$ ion structures, namely $[CH_3CNCH_3]^+$ ($\Delta_f H^\circ_{300} = 738 \pm 7$ kJ/mol⁶) and $[CH_2=CHCH=NH_2]^+$, **7** ($\Delta_f H^\circ_{300} = 747 \pm 7$ kJ/mol,^{6,16} a value comparable to a previous estimate of 735–774 kJ/mol¹⁷). The formation of $[CH_3CNCH_3]^+$ ions by dissociative ionization of **1n** can be reasonably excluded on the basis of simple mechanistic considerations. Thermochemical information is summarized in Figure 3.

The present AE measurement thus confirms the finding, established by collisional experiments,⁶ that $[C_3H_6N]^+$ ions from

(10) Lias, S. G.; Bartmess, J. E.; Liebman, J. F.; Holmes, J. L.; Levin, R. D.; Mallard, W. G. *Gas Phase Ion and Neutral Thermochemistry*. In *J. Phys. Chem. Ref. Data*, **1988**, *17*, Suppl. No. 1.

(11) Aue, D.; Bowers, M. T., Eds.; *Gas-Phase Ion Chemistry*; Academic Press: New York, 1979; Vol. 2, p 23.

(12) (a) Chupka, W. A. *J. Chem. Phys.* **1971**, *54*, 1936. (b) Guyon, P. M.; Berkowitz, J. *J. Chem. Phys.* **1971**, *54*, 1814.

(13) Stein, S. E.; Rabinovitch, B. S. *J. Chem. Phys.* **1973**, *58*, 2438.

(14) (a) Baer, T.; Morrow, J. C.; Shao, J. D.; Olesik, S. *J. Am. Chem. Soc.* **1988**, *110*, 5633. (b) Keister, J. W.; Riley, J. S.; Baer, T. *J. Am. Chem. Soc.* **1993**, *115*, 12613.

(15) Pedley, J. B.; Naylor, R. D.; Kirby, S. P. *Thermochemical Data of Organic Compounds*, 2nd ed.; Chapman & Hall: New York, 1986.

(16) Bouchoux, G.; Salpin, J. Y.; Leblanc, D.; Alcaraz, C.; Dutuit, O.; Palm, H. *Rapid Commun. Mass Spectrom.* **1995**, *9*, 1195.

(17) Stams, D. A.; Thomas, T. D.; MacLaren, D. C.; De, J.; Morton, T. H. *J. Am. Chem. Soc.* **1990**, *112*, 1427.

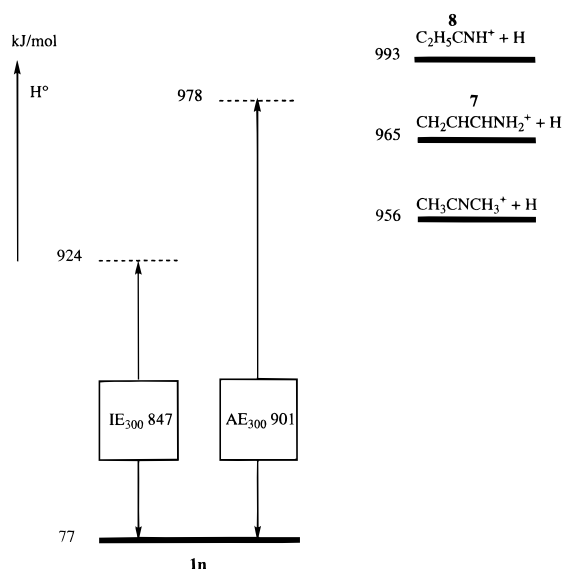
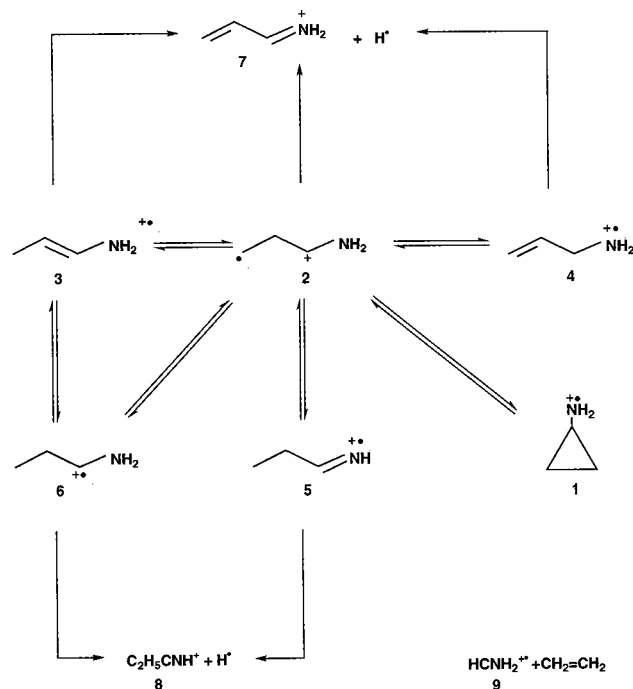


Figure 3. Enthalpy diagram showing relevant $\Delta_f H^\circ_{300}$ values and the two 300 K experimental thresholds for ionization and dissociation of cyclopropylamine.

Scheme 2



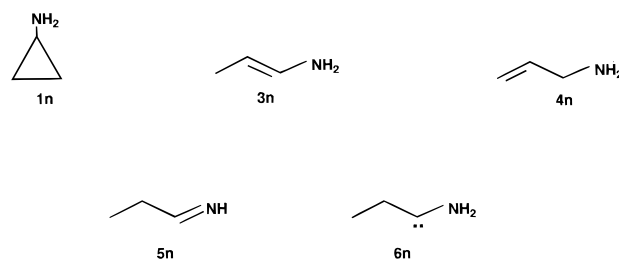
dissociative electron ionization of cyclopropylamine have the structure $[\text{CH}_2=\text{CHCH}=\text{NH}_2]^+$, **7**. Moreover it demonstrates that the dissociation occurs with an average excess energy 13 kJ/mol above the threshold for the product **7** + H^\bullet at 300 K.

B. Computational Results. An extensive investigation of the various possible isomerization/dissociation pathways of the $[\text{C}_3\text{H}_7\text{N}]^{+\bullet}$ ions having the CCCN skeleton has been undertaken with use of molecular orbital calculations. Scheme 2 summarizes the various mechanistic steps that have been considered.

Several *neutral* structures (Chart 2) were also investigated. Their energies provide estimates of ionization energies, which are presently unavailable, and allow us to address the question of the imine/enamine/aminocarbene tautomerism.

The following computational section is arranged into three parts, which separately discuss the features of stable neutral and

Chart 2



ionized structures, of isomerization processes, and of dissociations of $[\text{C}_3\text{H}_7\text{N}]^{+\bullet}$ ions including RRKM calculations.

(i) Stability of Neutral and Ionized $\text{C}_3\text{H}_7\text{N}$ Species. Relative energies of neutral cyclopropylamine (**1n**), allylamine (**4n**, $\text{CH}_2=\text{CHCH}_2\text{NH}_2$), 1-aminopropene (**3n**, $\text{CH}_3\text{CH}=\text{CHNH}_2$), propanimine (**5n**, $\text{CH}_3\text{CH}_2\text{CH}=\text{NH}$), and ethylaminocarbene (**6n**, $\text{CH}_3\text{CH}_2\text{CNH}_2$) have been estimated by molecular orbital calculations at the MP4SDTQ/6-311G(d,p)//MP2/6-31G(d)+ZPE level (Table 1). We note, in passing, that our theoretical results concerning the geometry of cyclopropylamine are in good agreement with the experimental structure determined by microwave spectroscopy.²⁰ The calculated energy ordering, **5n** < **3n** < **4n** < **1n** < **6n**, favors the propanimine structure **5n**. This observation illustrates the well-known stability order of the imine/enamine tautomeric pair.^{18,19} We note that the energy difference calculated here between enamine **3n** and imine **5n** (21 kJ/mol, Table 1) is comparable to what has been calculated for the two lower homologues, vinylamine $\text{CH}_2=\text{CHNH}_2$ and ethanimine $\text{CH}_3\text{CH}=\text{NH}$: 22 kJ/mol (MP4/6-311++G(d,p)//MP2/6-31G(d,p)+ZPE level¹⁸) and 16 kJ/mol (G2 level¹⁹).

Only two experimental heats of formation of gaseous $\text{C}_3\text{H}_7\text{N}$ molecules are known. For cyclopropylamine a value of $\Delta_f H^\circ_{300}$ (**1n**) = 77 kJ/mol has been reported;¹⁰ in the case of allylamine an incremental estimate gives $\Delta_f H^\circ_{300}$ (**4n**) = 55 kJ/mol.²¹ The difference in heat of formation points to a greater stability (22 kJ/mol) for allylamine with respect to cyclopropylamine. The present estimate is in reasonable agreement with the theoretical value of 16 kJ/mol. The calculated 300 K relative energies (Table 1) combined with the experimental heats of formation of **1n** and **4n** allow the following estimates: $\Delta_f H^\circ_{300}$ (**5n**) = 10 kJ/mol, $\Delta_f H^\circ_{300}$ (**3n**) = 30 kJ/mol, and $\Delta_f H^\circ_{300}$ (**6n**) = 160 kJ/mol.

Five of the radical cations displayed in Scheme 2 represent local minima on the $[\text{C}_3\text{H}_7\text{N}]^{+\bullet}$ surface, namely structures **2**–**6**. All attempts to optimize the geometry of ionized cyclopropylamine **1** failed and, instead, led to the open structure **2**. The stability ordering of these ionized species is in contrast with their neutral counterparts. The most stable ion is ionized 1-aminopropene, **3**. The distonic isomer **2**, ionized ethylamino carbene **6**, and ionized allylamine **4** are situated 65, 109, and 138 kJ/mol, respectively, above **3**. Finally structure **5** is the most energetic isomer, while its neutral counterpart was the most stable of the investigated $\text{C}_3\text{H}_7\text{N}$ structures. The reversed order of stability between **5n** and **3n** (21 kJ/mol) and between **3** and **5** (147 kJ/mol) is remarkable. The situation appears to be more pronounced than has been observed for the lower homologues ($\text{CH}_3\text{CH}=\text{NH} \rightarrow \text{CH}_2=\text{CHNH}_2$: 16–22 kJ/mol; $[\text{CH}_2=\text{CH}$

(18) Bouchoux, G.; Penaud-Berruyer, F.; Nguyen, M. T. *J. Am. Chem. Soc.* **1993**, *115*, 9728.

(19) Lammertsma, K.; Prasad, V. *J. Am. Chem. Soc.* **1994**, *116*, 642.

(20) Rall, M.; Harmony, M. D.; Cassada, D. A.; Staley, S. W. *J. Am. Chem. Soc.* **1986**, *108*, 6184.

(21) Benson, S. W. *Thermochemical kinetics*, 2nd ed.; Wiley: New York, 1976.

$\text{NH}_2]^+ \rightarrow [\text{CH}_3\text{CH}=\text{NH}]^{+\bullet}$: 124 kJ/mol),¹⁸ or with the corresponding oxygenated species ($\text{CH}_3\text{CH}_2\text{CHO} \rightarrow \text{CH}_3\text{CH}=\text{CHOH}$: 17 kJ/mol; $[\text{CH}_3\text{CHCHOH}]^{+\bullet} \rightarrow [\text{CH}_3\text{CH}_2\text{CHO}]^{+\bullet}$: 91²⁴ to 108 kJ/mol).¹⁰ This may be due to a better stabilization of the radical cation **3** by the combined effect of the methyl and amino groups on the radical and the charged sites, respectively.

Three points of comparison are possible between the experimental and theoretical thermochemistry of $[\text{C}_3\text{H}_7\text{N}]^{+\bullet}$ ions in Scheme 2: ionized allylamine, **4**, and the sets of fragments $[\text{CH}_2=\text{CHCH}=\text{NH}_2]^+ (7) + \text{H}^\bullet$ and $[\text{CH}_3\text{CH}_2\text{CNH}]^+ (8) + \text{H}^\bullet$. The 300 K heat of formation of ionized allylamine **4** (905 ± 5 kJ/mol, using $\Delta_f H^\circ_{300}(\text{allylamine}) = 55$ kJ/mol²¹ and $\text{IE}(\text{allylamine}) = 8.76^{10}$ to 8.85 eV¹¹) is ca. 60 kJ/mol below the fragments **7** + H^\bullet (using $\Delta_f H^\circ_{300}[\text{CH}_2=\text{CHCH}=\text{NH}_2]^+ = 747$ kJ/mol¹⁶ and $\Delta_f H^\circ_{300}(\text{H}^\bullet) = 218$ kJ/mol¹⁰). The computation gives a slightly lower difference in energy of 47 kJ/mol at 0 K and of 49 kJ/mol at 300 K. The experimental difference in $\Delta_f H^\circ_{300}$ between **7** and **8** is equal to 28 kJ/mol ($\Delta_f H^\circ_{300}[\text{CH}_3\text{CH}_2\text{CNH}]^+ = 775$ kJ/mol¹⁰). Our calculation gives an energy difference of 23 kJ/mol at both 0 and 300 K (Table 1), in good agreement with experiment. These comparisons may be used to propose a heat of formation for the various $[\text{C}_3\text{H}_7\text{N}]^{+\bullet}$ ions. Considering the calculated 300 K relative energies of the relevant $[\text{C}_3\text{H}_7\text{N}]^{+\bullet}$ ions and the experimental $\Delta_f H^\circ_{300}$ of **4**, **7**, and **8**, we propose the following heats of formation: $\Delta_f H^\circ_{300}(\mathbf{2}) = 840$ kJ/mol, $\Delta_f H^\circ_{300}(\mathbf{3}) = 770$ kJ/mol, $\Delta_f H^\circ_{300}(\mathbf{5}) = 922$ kJ/mol, and $\Delta_f H^\circ_{300}(\mathbf{6}) = 884$ kJ/mol.

In the case of **1** no $\Delta_f H^\circ_{300}$ can be calculated because of the unstability of ionized cyclopropylamine predicted by the calculation. An estimate of the energy required by a vertical ionization may be proposed however using the total energy calculated for the radical cation assuming the geometrical parameters of the neutral molecule **1n** (line denoted **1** (vertical) in Table 1). The value $\text{IE}_{\text{vcalc}} = 9.48$ eV is in good agreement with the vertical ionization energy determined from the photoelectron spectrum, $\text{IE}_{\text{vexp}} = 9.44$ eV.¹¹ The experimental adiabatic IE_a value of 8.70–8.85 eV^{10,11} is clearly lower than IE_v . This difference may be ascribed to a substantial Franck–Condon effect in ionization of cyclopropylamine as already observed for other nitrogen molecules.^{11,23} Theoretical results suggest that ionized cyclopropylamine is not a stable structure but spontaneously rearranges by ring opening to the distonic ion **2**. Thus, the ionization process would give rise to an unstable cyclic species which, in turn, relaxes to structure **2**. At 300 K, the ionization threshold generates $[\text{C}_3\text{H}_7\text{N}]^{+\bullet}$ ions situated 41 kJ/mol below **7** + H^\bullet (Figure 3). Considering the previous estimate of $\Delta_f H^\circ_{300}(\mathbf{2}) = 840$ kJ/mol and the calculated contribution to enthalpy at 300 K for this species (Table 1), the appearance of the molecular ions is associated with an excess energy of ca. 94 kJ/mol above the ground state of **2**. After relaxation and according to the theoretical results, it must correspond to vibrationally excited **2** or to one of its isomers **3–6** (or to a mixture of them). This situation may be clarified by considering the various isomerization reactions of ion **2** and their energy requirements, as described below.

(ii) Isomerization of the Distonic Ion 2. The distonic ion **2** may undergo rearrangement into the four entities **3–6** via 1,2-, 1,3-, or 1,4-hydrogen migrations (Scheme 2). The seven isomerization reactions considered fall into two categories: high

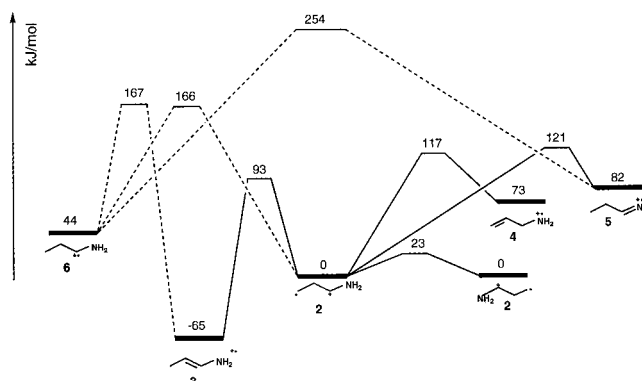
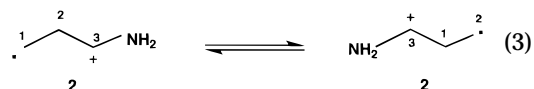


Figure 4. Calculated (PUMP4SDTQ/6-311G**//UMP2/6-31G*+ZPE) potential energy profile for isomerizations of $[\text{C}_3\text{H}_7\text{N}]^{+\bullet}$ ions.

energy processes involving the ethylaminocarbene **6** (for which the transition structures **2/6**, **3/6**, and **5/6** lie in the 160–260 kJ/mol relative energy range) and low energy processes involving ions **3–5** and transition structures (**2/3**, **2/4**, and **2/5**, situated between 90 and 120 kJ/mol above **2**). A schematic potential energy profile illustrating these various reactions is presented in Figure 4.

Note in particular that the degenerate rearrangement $\mathbf{2} \rightleftharpoons \mathbf{2}$ via a 1,2- HCNH_2 migration (eq 3) turns out to be the isomerization process with the lowest energy requirement.



This reaction is found to correspond to a critical energy of only 23 kJ/mol. The transition structure **2/2** (Chart 1) is characterized by a $\text{C}(1)\text{C}(2)=\text{C}(1)\text{C}(3)$ bond length of 1.597 Å and a $\text{C}(2)\text{C}(3)$ bond length of 1.442 Å (compare to the corresponding value of 1.494 and 1.500 Å respectively in **1n**) and by a planar disposition of the HCNH_2 moiety (which is also in contrast with the geometry of **1n**). From a mechanistic point of view the reversibility of the process $\mathbf{2} \rightleftharpoons \mathbf{2}$ implies a complete equivalency between the two methylene groups of the distonic ion **2**.

It is clear that upon ionization of neutral cyclopropylamine, **1n**, several isomerization reactions of **2** are allowed even at threshold. In this particular energy regime it has been previously estimated that **2** possesses an amount of internal energy of 94 kJ/mol above its ground state. Consequently **2** may isomerize via reaction $\mathbf{2} \rightleftharpoons \mathbf{2}$, but probably also via $\mathbf{2} \rightleftharpoons \mathbf{3}$.

(iii) Dissociation by H Atom Loss. Two sets of fragments $[\text{CH}_2\text{CHCHNH}_2]^+, \mathbf{7} + \text{H}^\bullet$ and $[\text{CH}_3\text{CH}_2\text{CNH}]^+, \mathbf{8} + \text{H}^\bullet$ have been considered as possible dissociation products from ions **1–6** in Scheme 2. As discussed in the Experimental Section, the measured threshold energy for $[\text{C}_3\text{H}_6\text{N}]^+$ fragment ions is only compatible with product **7**. It has been established that the appearance energy of the $[\text{C}_3\text{H}_6\text{N}]^+$ fragment ions corresponds, at 300 K, to an energy level situated 13 kJ/mol above **7** + H^\bullet (Figure 3). After correction based on the ZPE and STE estimates presented in Table 1, this means that dissociation occurs with an excess energy of 30 kJ/mol above the vibrational ground state of **7**. This corresponds to ion **2** containing ca. 150 kJ/mol of internal energy above its vibrational ground state.

According to molecular orbital calculations, at this energy level, the isomerizations $\mathbf{2} \rightarrow \mathbf{4}$ and $\mathbf{2} \rightarrow \mathbf{5}$ and the three dissociation pathways $\mathbf{2} \rightarrow \mathbf{7} + \text{H}^\bullet$, $\mathbf{3} \rightarrow \mathbf{7} + \text{H}^\bullet$, and $\mathbf{4} \rightarrow \mathbf{7} + \text{H}^\bullet$ are opened in addition to the degenerate rearrangement $\mathbf{2} \rightleftharpoons \mathbf{2}$.

(22) (a) Pople, J. A.; Scott, A. P.; Wong, M. W.; Radom, L. *Isr. J. Chem.* **1993**, 33, 345. (b) Scott, A. P.; Radom, L. *J. Phys. Chem.* **1996**, 100, 16502.

(23) Shaffer, S. A.; Turecek, F.; Cerny, R. L. *J. Am. Chem. Soc.* **1993**, 115, 12117.

(24) Turecek, F.; Cramer, C. J. *J. Am. Chem. Soc.* **1995**, 117, 12243.

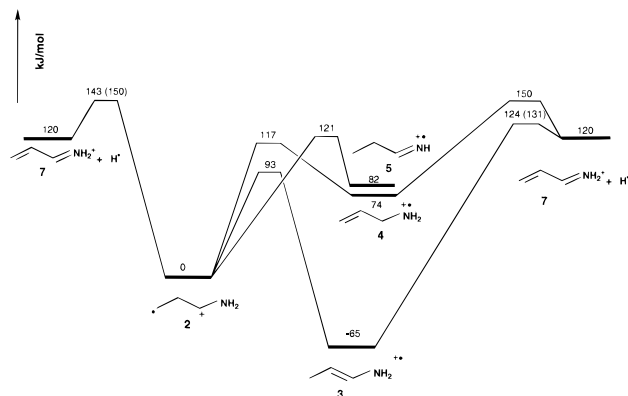


Figure 5. Calculated PUMP4SDTQ/6-311G**//UMP2/6-31G*+ZPE potential energy profile (QCISD(T)/6-311G** results in parentheses) for dissociations of $[C_3H_7N]^+$ ions.

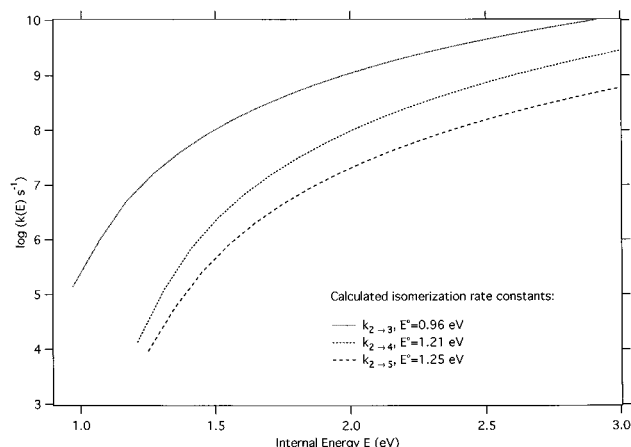


Figure 6. Calculated RRKM rate constants for isomerizations of $[C_3H_7N]^+$ ions.

2 and the isomerization route $2 \rightarrow 3$ (see Scheme 2 and the partial potential energy profile presented in Figure 5).

From this observation one may expect a considerable complexity for H atom loss: three competitive dissociation reactions preceded by a loss of identity of the hydrogen atoms and carbon atoms C(2) and C(3). No experimental evidence corroborates these predictions: the metastable peak is apparently not composite, pointing toward a unique dissociation process, and the deuterium borne by the nitrogen remains on this atom (under a detection limit of 2%). This latter point is explicable by the absence of the isomerization reaction $2 \rightarrow 5$ (leading to negligible formation of a structure able to eliminate a deuterium atom). To shed light upon these questions we have performed rate constant calculations using the statistical theory of unimolecular reactions (see the Appendix for the computational details).

Before considering the possibility of a competitive formation of the dissociation products $7 + H^\bullet$ from the three isomers **2**, **3**, and **4**, we first examine the individual isomerization rates for the isomerization reactions $2 \rightarrow 3$, $2 \rightarrow 4$, and $2 \rightarrow 5$. As indicated by the plots reported in Figure 6, the calculation predicts that $k_2 \rightarrow 3 > k_2 \rightarrow 4 > k_2 \rightarrow 5$ at all internal energies.

For example, the ratio of the calculated rate constants is equal to 98/1.7/0.3 at internal energy $E = 1.5$ eV and to 68/26/6 at $E = 4.0$ eV. It consequently appears that the competition largely favors the isomerization of the distonic ion **2** to ionized propenylamine **3**. The reactions $2 \rightarrow 4$ and especially $2 \rightarrow 5$ are negligible isomerization routes, particularly at low internal energy. The latter conclusion is in agreement with the

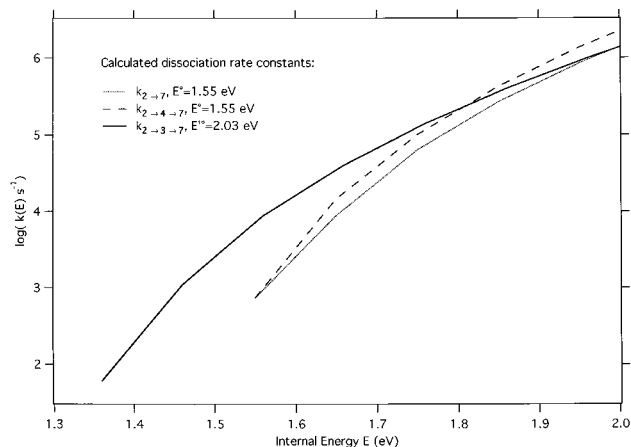


Figure 7. Calculated RRKM and experimental rate constants for dissociations of $[C_3H_7N]^+$ ions.

experimental observation of the virtually exclusive loss of H from ND₂-cyclopropylamine.

Considering now the three possible reaction paths leading to $7 + H^\bullet$, the rate constants reported in Figure 7 indicate that the process $2 \rightarrow 3 \rightarrow 7 + H^\bullet$ is the most favored for ions of internal energy up to ca. 2.0 eV. As expected from the similarity of the transition state structures and energies, the rate constant for the two-step process $2 \rightarrow 4 \rightarrow 7 + H^\bullet$ is of comparable magnitude to that of the direct dissociation $2 \rightarrow 7 + H^\bullet$ in the internal energy range considered.

A point which may also be noted is the reduced slope of the curve for $2 \rightarrow 3 \rightarrow 7 + H^\bullet$ when compared with the other two. This is due to the slow-down effect of the isomerization of **2** into the stable isomer **3** on the overall dissociation rate.

Consequently, the low energy behavior of ions **2** produced by ionization of cyclopropylamine appears to be dominated by the two-step reaction $2 \rightarrow 3 \rightarrow 7 + H^\bullet$, as displayed in Figure 7, and by the degenerate rearrangement $2 \rightleftharpoons 2$ (the low critical energy of this process renders its occurrence inescapable). This is expected to be true for metastable $[C_3H_7N]^+$ ions produced by ionization of cyclopropylamine, and also for those ions dissociating at threshold. These two points deserve some further comments.

The breakdown graph presented on Figure 2 may be used to derive the rate constant values in the vicinity of the dissociation onset. To a first approximation, the abundances of the parent $[C_3H_7N]^+$ and fragment $[C_3H_6N]^+$ ions, at a given internal energy E , are given by eq 4:

$$[C_3H_7N]^+ = [C_3H_7N]_0^+ \exp(-k(E)t_1) \quad (4a)$$

$$[C_3H_6N]^+ = [C_3H_7N]_0^+ (1 - \exp(-k(E)t_2)) \quad (4b)$$

where $k(E)$ is the dissociation rate constant and t_1 and t_2 the flight times of the parent and daughter ions, respectively. Under our experimental conditions, the time spent by the parent ions $[C_3H_7N]^+$ (m/z 57) between the ionization region and the detector (the maximum lifetime of the parent ions) is equal to $t_1 = 330 \pm 20 \mu s$. For the m/z 56 fragment ions, the corresponding flight time is equal to $t_2 = 290 \pm 20 \mu s$.

In principle, the $k(E)$ values may be deduced by numerical inversion of the relationships (4a) and (4b) by using the experimental fractional abundances presented in Figure 2. The uncertainty in $k(E)$ due to the experimental limitations on the measurement both of the flight times and of the ionic abundances must, however, be taken into account. The results are

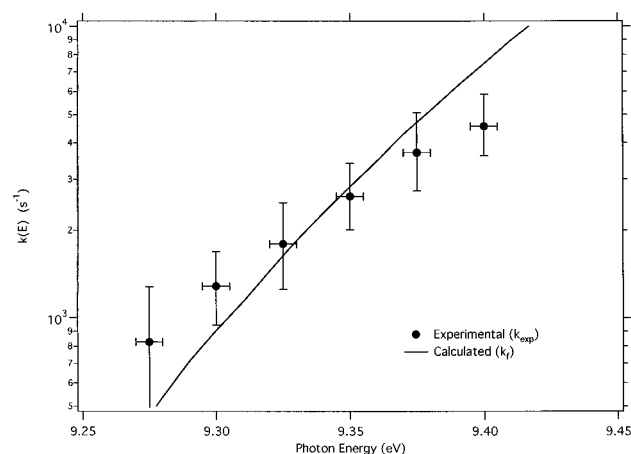


Figure 8. Experimental rate constant derived from the experimental breakdown graph presented in Figure 2 (k_{exp}) and overall dissociation rate constant calculated for $2 \rightarrow 3 \rightarrow 7 + \text{H}^\bullet$.

significant only for the threshold zone, i.e. for photon energies between 9.2 and 9.5 eV. The resulting data are presented in Figure 8.

A comparison between the experimentally derived rate constant values, k_{exp} , and the theoretical estimates based on RRKM calculations, $k_{2 \rightarrow 3 \rightarrow 7}$, is only possible if one may associate an internal energy value E with a given nominal photon energy. The internal energy of an ion in a coincidence experiment is well-defined, providing the ionization energy of the corresponding neutral gives a correct value for its radical cation. As underlined in the computational section, this is not the case for cyclopropylamine: its radical cation is unstable and the ionization leads to excited distonic ions **2**. There is unfortunately no direct experimental access to the relative energy of the latter with respect to neutral cyclopropylamine. A reasonable alternative may be suggested.

First of all, one may consider that the most representative rate constant value presented in Figure 8 corresponds to the crossover point (see Figure 2). Here it has been observed that (i) the nominal photon energy was equal to $C_{300} = 9.34$ eV and (ii) the corresponding internal energy content of distonic ions **2** was about 150 kJ/mol. The latter information is derived from a combination of ab initio calculations and reference to the known heat of formation of the products $7 + \text{H}^\bullet$ (see above). Consequently, the experimental and theoretical rate constant values may be compared if the energy scale E (the internal energy of ions **2**) is anchored to $E = 1.49$ eV for the nominal photon energy of 9.34 eV (i.e. photon energy (eV) = $E(\text{eV}) + 7.85$ (eV)). The calculated rate constant $k_{2 \rightarrow 3 \rightarrow 7}$ so adjusted is displayed beside the experimental points in Figure 8. The agreement between the theoretical rate constant $k_{2 \rightarrow 3 \rightarrow 7}$ and the experimental data k_{exp} is satisfactory, given the various approximations and simplifications inherent to the present treatment. In particular, the identical order of magnitude of both rate constants indirectly confirms the accurate estimation for the energetics of the process $2 \rightarrow 3 \rightarrow 7 + \text{H}^\bullet$. Moreover, the slope of the rate constant curve is reproduced and confirms that the slow rise of the rate constant observed in that system is actually due to the passage through a very stable isomerized structure, **3**, before dissociation.

The dissociation of $[\text{C}_3\text{H}_7\text{N}]^{+\bullet}$ (m/z 57) ions of lifetime $\approx 10^{-5}$ s (the metastable ions) corresponds to an internal energy E of ca. 1.7 eV (164 kJ/mol, Figure 7). In this energy regime the reaction $2 \rightarrow 3 \rightarrow 7 + \text{H}^\bullet$ is still faster than $2 \rightarrow 7 + \text{H}^\bullet$ or $2 \rightarrow 4 \rightarrow 7 + \text{H}^\bullet$. Consequently most of the ions **2** dissociate via

this single channel. The metastable peak measured by the MIKE technique is essentially noncomposite, in agreement with a single dissociation process. The KERD deduced from the analysis of the peak profile is centered around a single kinetic energy release value (see Figure 1). This situation corresponds to a nonstatistical distribution of the total excess energy of the dissociating species among its internal degrees of freedom. For the m/z 57 metastable ion, the excess internal energy above $7 + \text{H}^\bullet$ is equal to $E^* \approx 44$ kJ/mol, which consists of 11 kJ/mol of reverse critical energy (reaction $7 + \text{H}^\bullet \rightarrow 3$) and 33 kJ/mol of non-fixed energy. The experimental kinetic energy release T_{average} of 24 kJ/mol (250 meV, Figure 1) represents a large fraction of E^* , in keeping with a nonstatistical behaviour of the dissociating system.

Concluding Remarks

The behavior of cyclopropylamine under photon or electron ionization exhibits a chemistry peculiar to cation radical species. Molecular orbital calculation at the (PU)MP4SDTQ/6-311G**//MP2/6-31G*+ZPE level demonstrates that the cyclic structure of cyclopropylamine is not preserved after electron removal. The radical cation collapses to a more stable open form, which is a distonic ion. The dissociation of the latter by hydrogen atom loss is preceded by isomerization to ionized 1-aminopropene, the most stable of the $[\text{C}_3\text{H}_7\text{N}]^{+\bullet}$ ions possessing the CCCN skeleton. Thus the lowest energy route followed by the ions originating from ionization of cyclopropylamine is predicted to be $[\text{CH}_2\text{CH}_2\text{CH}=\text{NH}_2]^+$, $2 \rightarrow [\text{CH}_3\text{CH}=\text{CHNH}_2]^+$, $3 \rightarrow [\text{CH}_2=\text{CHCH}=\text{NH}_2]^+$, $7 + \text{H}^\bullet$. The degenerate rearrangement $[\text{CH}_2\text{CH}_2\text{CH}=\text{NH}_2]^+$, $2 \rightleftharpoons [\text{NH}_2=\text{CHCH}_2\text{CH}_2]^+$, 2 is also found to require a negligible critical energy.

These theoretical predictions are confirmed by the experiments. The dissociation threshold is compatible only with the fragment ion structure $[\text{CH}_2=\text{CHCH}=\text{NH}_2]^+$. The dissociation of metastable ions occurs via a single mechanism, in which the expelled hydrogen atom comes exclusively from the carbon positions. Finally, a statistical modeling of the dissociation rate agrees with the experimental rate constant derived from photoion-photoelectron coincidence measurements. Several thermochemical parameters, including the standard heat of formation of the neutrals and radical cations as well as the adiabatic ionization energies, have also been determined.

The spontaneous ring opening of cyclopropylamine upon electron removal demonstrated in the present study fully parallels the mechanism proposed for inactivation of monoamine oxidase^{4c} and confirms that the unstability of small ring cation radicals is an ubiquitous aspect of ionic chemistry in both the gas phase and the condensed phase.

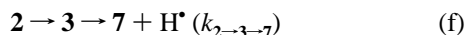
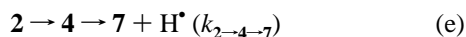
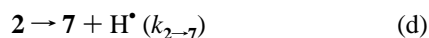
Appendix

RRKM calculation of unimolecular rate constants was performed by using the Stein–Rabinovitch algorithm¹³ to estimate the sums, $\sum P_i^\ddagger(E - E_0)$, and the densities, $N_f(E)$, of vibrational states. The normal mode frequencies given by molecular orbital calculations (HF/6-31G* scaled by a factor of 0.89^{22b}) were used in these calculations, and torsional modes were treated as low-frequency vibrations.

The critical energies were inferred from the PUMP4SDTQ- (or QCISD(T) when available, Table 1) 6-311G(d,p)//MP2/6-31G(d)+ZPE calculations. The following isomerization reactions:



and dissociation processes



have been considered.

The internal energy dependences of the calculated rate constants for the isomerization reactions $2 \rightarrow 3$, $2 \rightarrow 4$, and $2 \rightarrow 5$ are displayed in Figure 6.

The direct fragmentation of the distonic ion **2** is associated with a single rate constant $k_{2 \rightarrow 7}$ given by

$$k_{2 \rightarrow 7} = \sum P_{27}^{\ddagger}(E - E_0)/hN_2(E) \quad (5)$$

The use of a critical energy value $E_0 = 1.55$ eV as indicated by the QCISD(T) calculation leads to the $k_{2 \rightarrow 7}$ curve presented on Figure 7.

The overall rate constant for the two-step process $2 \rightleftharpoons 4 \rightarrow 7$, $k_{2 \rightarrow 4 \rightarrow 7}$ is given by the steady-state expression

$$k_{2 \rightarrow 4 \rightarrow 7} = (k_{4 \rightarrow 7}k_{2 \rightarrow 4})/(k_{2 \rightarrow 4} + k_{4 \rightarrow 2} + k_{4 \rightarrow 7}) \quad (6)$$

where the $k_{i \rightarrow j}$ represents the elementary rate constants for the $i \rightarrow j$ reactions. Among the three elementary steps, the most favored is the isomerization $4 \rightarrow 2$ which needs only 43 kJ/mol, as compared to 76 and 117 kJ/mol for $4 \rightarrow 7$ and $2 \rightarrow 4$,

respectively. Thus, in a first approximation, we can consider that $k_{4 \rightarrow 2} \gg k_{2 \rightarrow 4}$, thus leading to:

$$k_{2 \rightarrow 4 \rightarrow 7} = [\sum P_{47}^{\ddagger}(E - E_{0a})/hN_2(E)] [\sum P_{24}^{\ddagger}(E - E_{0b}) / (\sum P_{47}^{\ddagger}(E - E_{0a}) + \sum P_{24}^{\ddagger}(E - E_{0b}))] \quad (7)$$

and, if the inequality $k_{4 \rightarrow 2} \gg k_{4 \rightarrow 7}$ also holds:

$$k_{2 \rightarrow 4 \rightarrow 7} = \sum P_{47}^{\ddagger}(E - E_{0a})/hN_2(E) \quad (8)$$

Using the critical energy values $E_{0a} = 1.55$ eV (150 kJ/mol) and $E_{0b} = 1.21$ eV (117 kJ/mol) it appears that the latter approximation is valid to within ca. 1%. The resulting rate constant calculated under these simplifications is reported in Figure 7.

Finally, it remains to investigate the overall process $2 \rightleftharpoons 3 \rightarrow 7$. For this reaction the observed decay rate is of the form

$$k_{2 \rightarrow 3 \rightarrow 7} = (k_{3 \rightarrow 7}k_{2 \rightarrow 3})/(k_{2 \rightarrow 3} + k_{3 \rightarrow 2} + k_{3 \rightarrow 7}) \quad (9)$$

Due to the high stability of **3** with respect to **2** we observe that $k_{2 \rightarrow 3}$ is much greater than $k_{3 \rightarrow 2}$ or $k_{3 \rightarrow 7}$. Thus $k_{2 \rightarrow 3 \rightarrow 7}$ reduces to

$$k_{2 \rightarrow 3 \rightarrow 7} \approx k_{3 \rightarrow 7} = \sum P_{37}^{\ddagger}(E' - E'_0)/hN_3(E') \quad (10)$$

with the internal energy E' of ions **3** related to the internal energy E of ions **2** by $E' = E + 65$ kJ/mol and with $E'_0 = 196$ kJ/mol (2.03 eV, QCISD(T) result).

Acknowledgment. The authors would like to thank the staff of the Laboratoire pour l'Utilisation du Rayonnement Electromagnétique (LURE) for operating the storage ring and general facilities during the experiments. M.T.N. thanks the Funds for Scientific Research (FWO-Vlaanderen) and KU Leuven Research Council (GOA) for continuing support.

JA971724M